1076–1083 *Nucleic Acids Research, 1998, Vol. 26, No. 4*

2-Aminopurine as a fluorescent probe for DNA base flipping by methyltransferases

Birgit Holz, Saulius Klimasauskas[1], Saulius Serva[1] and Elmar Weinhold*

Max-Planck-Institut für Molekulare Physiologie, Abteilung Physikalische Biochemie, Rheinlanddamm 201, D-44139 Dortmund, Germany and [1]Institute of Biotechnology, Graiciuno 8, LT-2028 Vilnius, Lithuania

Received September 19, 1997; Revised and Accepted December 22, 1997

ABSTRACT

DNA base flipping, which was first observed for the C5-cytosine DNA methyltransferase M·*Hha*I, results in a complete removal of the stacking interactions between the target base and its neighbouring bases. We have investigated whether duplex oligodeoxynucleotides containing the fluorescent base analogue 2-aminopurine can be used to sense DNA base flipping. Using M·*Hha*I as a paradigm for a base flipping enzyme, we find that the fluorescence intensity of duplex oligodeoxynucleotides containing 2-aminopurine at the target site is dramatically enhanced (54-fold) in the presence of M·*Hha*I. Duplex oligodeoxynucleotides containing 2-aminopurine adjacent to the target cytosine show little fluorescence increase upon addition of M·*Hha*I. These results clearly demonstrate that duplex oligodeoxynucleotides containing 2-aminopurine at the target site can serve as fluorescence probes for base flipping. Another enzyme hypothesized to use a base flipping mechanism is the N6-adenine DNA methyltransferase M·*Taq*I. Addition of M·*Taq*I to duplex oligodeoxynucleotides bearing 2-aminopurine at the target position, also results in a strongly enhanced fluorescence (13-fold), whereas addition to duplex oligodeoxynucleotides containing 2-aminopurine at the 3′- or 5′-neighbouring position leads only to small fluorescence increases. These results give the first experimental evidence that the adenine-specific DNA methyltransferase M·*Taq*I also flips its target base.

INTRODUCTION

Specific binding of proteins to DNA often leads to drastic conformational changes in the DNA structure. Proteins can bend, kink, unwind and melt the DNA or can flip out a whole base (nucleotide) from the double helix. Base flipping was initially observed by X-ray crystallography for the C5-cytosine DNA methyltransferase from *Haemophilus haemolyticus* (M·*Hha*I) (1). Subsequently, a second C5-cytosine DNA methyltransferase, from *Haemophilus aegypticus* (M·*Hae*III) (2), the thymidine dimer excision repair enzyme endonuclease V (3) and the uracil DNA glycosylase (4) were seen to use a base flipping mechanism. In all four protein–DNA complexes a base is completely rotated out of the DNA double helix. The C5-cytosine DNA methyltransferases and the uracil DNA glycosylase have their target bases flipped out of the DNA helix into a cleft within each enzyme, where catalysis takes place. In contrast, with endonuclease V one of the partner adenines of the thymidine dimer is flipped into a hydrophobic pocket of the enzyme permitting the catalytic residues to reach the target thymidine dimer. In all these cases base flipping allows the catalytic machinery to gain access to the target site within the bulky DNA substrate.

It has been postulated that base flipping occurred early in evolution and that it might be found in many DNA modifying enzymes (5). Possible candidates are other C5-cytosine DNA methyltransferases, N6-adenine and N4-cytosine DNA methyltransferases as well as DNA glycosylases and DNA repair enzymes. This hypothesis is supported by a number of X-ray structures of enzymes, which have been crystallized without their DNA substrates. The catalytic sites of O6-methylguanine DNA methyltransferase (6), β-glucosyl transferase (7), exonuclease III (8), photolyase (9), endonuclease III (10), DNA 3-methyl adenine glycosylase II (11,12) and N4-cytosine DNA methyltransferase M·*Pvu*II (13) were all found in the interior of the proteins. In each instance, base flipping appears to be necessary to bring the active site amino acid residues in close proximity to the target deoxynucleotide.

A similar example is the N6-adenine DNA methyltransferase from *Thermus aquaticus* (M·*Taq*I), which catalyses the methyl group transfer from *S*-adenosyl-L-methionine (AdoMet) to the exocyclic amino group of adenine within the double-stranded (ds) 5′-TCGA-3′ DNA sequence (14). The structure of M·*Taq*I in complex with its cofactor consists of two domains which form a cleft wide enough to accommodate dsDNA (15). However, modelling of B-DNA into the M·*Taq*I structure showed that the distance between the target adenine and the activated methyl group of the cofactor is 15 Å, which is too large for direct methyl group transfer (16). By rotating the adenine out of the DNA helix towards the cofactor, the distance between the methyl group donor and acceptor can be significantly reduced, and hence a base flipping mechanism was proposed for M·*Taq*I. A structural comparison of M·*Taq*I with the base flipping C5-cytosine DNA methyltransferase M·*Hha*I showed that the catalytic domains of both enzymes have a very similar fold (17), although primary structural similarities between the two enzymes are limited to a few sequence motifs (18,19). In a superimposition of the catalytic domains of M·*Taq*I and M·*Hha*I both the cofactors and the catalytic motifs (N/D P P Y/F/W-motif for N6-adenine DNA methyltransferases and PC-motif for C5-cytosine DNA methyl-

*To whom correspondence should be addressed. Tel: +49 231 1206 357; Fax: +49 231 1206 229; Email: elmar.weinhold@mpi-dortmund.mpg.de

transferases) overlay very well (17). Because of the similar architecture of their catalytic domains a shared base flipping mechanism seems likely.

In general, X-ray crystallography of protein–DNA complexes provides the absolute proof of DNA base flipping. However, cocrystallization of proteins with their DNA substrates is often cumbersome, and in some cases cocrystals might never be obtained. Therefore, other methods suitable to detect DNA base flipping would be of great value. Recently, tighter binding of the two C5-cytosine DNA methyltransferases M·*Hha*I and M·*Hpa*II to duplex oligodeoxynucleotides containing mismatched bases at their target sites (20,21) and of the N6-adenine DNA methyltransferase M·*Eco*RV to duplexes containing unnatural bases with reduced hydrogen bonding capabilities at the target site (22) was reported. An alternative approach to detect base flipping might use the fluorescent base analogue 2-aminopurine. This base is a very sensitive probe to detect conformational changes in DNA structure (23), and it can be incorporated into oligodeoxynucleotides by solid phase DNA synthesis (24–28). The 2-aminopurine fluorescence is highly quenched in polynucleotides (29), due to stacking interactions with neighbouring bases (30,31) and would be expected to increase dramatically if the 2-aminopurine base is flipped out of the DNA helix. Furthermore, the 2-aminopurine fluorescence excitation and emission maxima are well separated from those of tryptophan and tyrosine residues in proteins, increasing its usefulness for studying protein–DNA interactions. Duplex oligodeoxynucleotides containing 2-aminopurine have been used to study the Klenow fragment of DNA polymerase I (32,33), T4 DNA polymerase (34–36), T7 RNA polymerase (37–39), *Escherichia coli* RNA polymerase (40) and helicases (41,42). Recently, duplex oligodeoxynucleotides containing 2-aminopurine have been used to study the N6-adenine DNA methyltransferase M·*Eco*RI, and a DNA base flipping mechanism was suggested for this enzyme (43).

Using the C5-cytosine DNA methyltransferase M·*Hha*I as a paradigm for a base flipping enzyme, we demonstrate that 2-aminopurine incorporated in DNA serves as an excellent spectroscopic probe for DNA base flipping. M·*Hha*I recognizes the specific tetranucleotide DNA sequence 5′-GCGC-3′ (44) and catalyses the methyl group transfer from AdoMet to the 5-position of the first cytosine (45). Titration with M·*Hha*I of a duplex oligodeoxynucleotide, in which the first cytosine is replaced with 2-aminopurine, yields a large increase in the 2-aminopurine fluorescence intensity. In addition, the N6-adenine DNA methyltransferase M·*Taq*I, which was suggested to use a base flipping mechanism, also shows a strongly enhanced 2-aminopurine fluorescence after addition to a duplex oligodeoxynucleotide, in which the target adenine is replaced by 2-aminopurine. Thus, duplex oligodeoxynucleotides containing 2-aminopurine can serve as spectroscopic probes for DNA base flipping in protein–DNA complexes. In addition, these duplex oligodeoxynucleotides should be very useful to study the dynamics of DNA base flipping.

MATERIALS AND METHODS

UV absorption spectra were measured in H_2O using a Varian Cary 3E spectrometer. HPLC was performed using a Beckmann System Gold equipped with a programmable solvent module 125, a diode array detector module 168, an analog interface module 406 and a Shimadzu spectrofluorometric detector RF-551. Fluorescence data were collected with a SLM-Aminco AB2 spectrofluorometer. The excitation and emission bandwidths were adjusted to 2 and 8 nm, respectively. Displayed emission spectra were corrected for lamp intensity fluctuations. Fluorescence titrations were performed with an excitation wavelength of 320 nm and an emission wavelength of 381 nm to lower the influence of the natural DNA base absorption and the protein tryptophan fluorescence. Emission spectra were recorded with an excitation wavelength of 320 nm. Due to the optical arrangement of the SLM AB2 all 2-aminopurine emission spectra show an extra shoulder at around 380 nm.

Oligodeoxynucleotide synthesis, purification and evaluation

Oligodeoxynucleotides were synthesized on an Applied Biosystems 392 DNA/RNA synthesizer, using standard β-cyanoethyl phosphoramidite chemistry or were purchased from MWG Biotech. 2-Aminopurine, C5-methylcytosine and N6-methyladenine phosphoramidites were purchased from Glen Research. Phosphoramidites for the normal bases and the synthesizer chemicals were obtained from Applied Biosystems and MWG Biotech. Phosphoramidites were dissolved manually in dry acetonitrile at 0.1 M concentration. Sequences of synthesized oligodeoxynucleotides are given in Table 1.

Evaluation of the coupling yield using the dimethoxytrityl cation assay gave an average of 98.5% per step. Deblocking was achieved by heating in aqueous ammonia (33%, Baker) at 55°C for 8 h. Syntheses were performed ‘trityl on’, and oligodeoxynucleotides containing the dimethoxytrityl group were purified by reversed phase HPLC (Hypersil ODS, 5 µm, 120 Å, 250 × 8 mm column, Bischoff) with a linear acetonitrile gradient (13–31% in 20 min, 2.5 ml/min) in triethylammonium acetate buffer (0.1 M, pH 7.0). After detritylation with acetic acid (80%) and ethanol precipitation oligodeoxynucleotides were desalted by gel filtration (NAP column, Pharmacia). Concentrations of oligodeoxynucleotides were determined by UV absorbance at 260 nm using the sum of the extinction coefficients of the individual bases.

Base composition of oligodeoxynucleotides was analysed by enzymatic digestion with snake venom phosphodiesterase and alkaline phosphatase followed by analytical reversed phase HPLC (26,46). Normalized peak areas of UV absorption at 254 nm correlated well with the expected base composition of the individual oligodeoxynucleotides. Oligodeoxynucleotides were 5′-labelled by treatment with T4 polynucleotide kinase (New England Biolabs) and [γ-^{32}P]ATP (0.4 MBq/µl, Hartmann Analytik) and analysed by denaturing PAGE. Radioactivity was quantified using a Phosphoimager (Molecular Imager System GS 525, Bio-Rad). All oligodeoxynucleotides showed a purity >95%.

DNA methyltransferases

M·*Hha*I was essentially isolated as described earlier (47); exhaustive dialysis prior to chromatography yielded AdoMet-free enzyme. The enzyme was purified to homogeneity by passing it through a pre-column of Q-Sepharose followed by column chromatography on S-Sepharose.

M·*Taq*I was expressed in ER 2267 *Escherichia coli* cells (New England Biolabs) harbouring pAGL15-M13, which carries the gene for M·*Taq*I under the inducible tac-promotor. pAGL15-M13 was kindly provided by Drs Jack Benner and Cheryl Baxa, New England Biolabs. Cells were grown at 37°C to an optical density of 0.6 at 600 nm and induced with IPTG (0.1 mM final concentration). After induction (4 h) cells were harvested by centrifugation (30 min at

3500 r.p.m.) and lysed by sonication in buffer A (Mes/HEPES/sodium acetate buffer mix, 6.7 mM each, pH 7.5, 1 mM EDTA, 10 mM β-mercaptoethanol and 10% glycerol), containing sodium chloride (200 mM) and phenylmethylsulfonyl fluoride (25 mg/l). After centrifugation (1 h at 35 000 *g*) the supernatant was loaded onto a cation exchange column (Poros HS/M, 26 × 95 mm, Perseptive Biosystems) and M·*Taq*I was eluted with a linear gradient of sodium chloride (0.2–1.0 M) in buffer A. Fractions containing M·*Taq*I were pooled, 3-fold diluted with buffer A and loaded onto a heparin column (heparin Sepharose CL 6B, 26 × 95 mm, Pharmacia). M·*Taq*I was eluted with a linear gradient of sodium chloride (0.2–1.0 M) in buffer A. Fractions containing M·*Taq*I were pooled, and the protein solution was concentrated by ultrafiltration (Centriprep 10, Amicon). The concentrated protein solution (10 ml) was loaded onto a gel filtration column (Superdex 75, 26 × 600 mm, Pharmacia) and eluted with a Tris–HCl buffer (20 mM, pH 7.4) containing potassium chloride (600 mM), EDTA (0.2 mM), DTE (2 mM) and glycerol (10%). Fractions containing M·*Taq*I were pooled, 2-fold diluted with glycerol and stored at –20°C. M·*Taq*I was at least 95% pure as judged by polyacrylamide gel electrophoresis in the presence of sodium dodecyl sulfate (48) and staining with Coomassie Blue. However, it was found that some fraction of the protein still contained the cofactor AdoMet. AdoMet bound to M·*Taq*I was removed as previously described (49).

Concentrations of M·*Hha*I and M·*Taq*I were estimated by the method of Bradford (50) (Coomassie Protein Assay Reagent, Pierce) using bovine serum albumin as standard. Concentrations were calculated using molecular weights of 37 100 g/mol for M·*Hha*I and 47 900 g/mol for M·*Taq*I.

Gel mobility shift assays

DNA binding studies with M·*Hha*I were performed by incubating M·*Hha*I (50 nM) with 5′-^{32}P-labelled duplexes oligodeoxynucleotides (5 nM) in buffer B (10 mM Tris–HCl, pH 7.4, 50 mM sodium chloride, 0.5 mM EDTA and 2 mM β-mercaptoethanol) supplied with glycerol (5%) and, where applicable, *S*-adenosyl-L-homocysteine (100 μM) for 30 min at 8°C. Aliquots (5 μl) were loaded onto a non-denaturing polyacrylamide gel (13%, acrylamide: bisacrylamide = 19:1) and electrophoresis was carried out in Tris–borate (45 mM, pH 8.3) and EDTA (1 mM) at 8°C for 2 h. Dried gels were autoradiographed to an X-ray film and the films were scanned with a ScanMaker E_6 densitometer (Microtek). DNA binding of M·*Taq*I was analysed by incubation of M·*Taq*I (30 nM) with 5′-^{32}P-labelled duplexes oligodeoxynucleotides (1 nM) in buffer C (10 mM Tris–acetate, pH 7.9, 50 mM potassium acetate, 10 mM magnesium acetate, 1 mM DTT and 0.01% Triton X-100) supplied with BSA (0.1 mg/ml) and glycerol (10%) at 0°C for 10 min. Aliquots (10 μl) were loaded onto a non-denaturing polyacrylamide gel (10%, acrylamide: bisacrylamide = 19:1) and electrophoresis was carried out in a buffer (pH 8.5) containing Tris–HCl (25 mM), glycine (192 mM) and EDTA (1 mM) at 0°C for 2 h. Radioactivity in the gel was visualized by autoradiography using a Bio-Rad Phosphoimager.

Steady-state fluorescence measurements

Fluorescence measurements were performed in 5 × 5 mm cuvettes at 25°C. Titrations of duplex oligodeoxynucleotides (20 and 250 nM) with M·*Hha*I were performed in buffer B and with M·*Taq*I in buffer C (see gel mobility shift assays). *S*-adenosyl-L-homocysteine (50 μM) was added to buffer B for titrations of 2**C**GC and G**C**2G with M·*Hha*I. Duplex oligodeoxynucleotides were made by mixing strands containing 2-aminopurine or non-fluorescent control strands with a 1.1-fold molecular excess of methylated complementary strands in the appropriate buffer and heating at 95°C for 2 min followed by cooling to room temperature over a period of 4 h. Enzymatic digestion of the duplex oligodeoxynucleotide G**2**GC was done by addition of DNase I (0.1 μg, Boehringer Mannheim) and snake venom phosphodiesterase (2 μg, Boehringer Mannheim) to a solution (400 μl) containing G**2**GC (250 nM) and buffer B supplemented with magnesium chloride (5 mM).

Table 1. Sequences of duplex oligodeoxynucleotides and their abbreviations used in this publication[a]

(i) Duplex oligodeoxynucleotides for M·*Hha*I					
5′-GACTGGTACAGTATCAG	x	**y**	z	C	TGACCCACAACATCCG-3′
3′-TGACCATGTCATAGTC	C	G	C^{Me}	G	ACTGGGTGTTGTAGGCT-5′
x	**y**	z			abbreviation
G	**C**	G			G**C**GC
2	**C**	G			2**C**GC
G	**2**	G			G**2**GC
G	**C**	2			G**C**2C
G	**A**	G			G**A**GC
(ii) Duplex oligodeoxynucleotides for M·*Taq*I					
5′-GCTGTTGAGATCCAGT	T	C	x	**y**	zGTAACCCACTCGTGC-3′
3′-CGACAACTCTAGGTCA	A^{Me}	G	C	T	TCATTGGGTGAGCACG-5′
x	**y**	z			abbreviation
G	**A**	A			TCG**A**
2	**A**	A			TC2**A**
G	**2**	A			TCG**2**
G	**A**	2			TCG**A**2

[a]The bases targeted by M·*Hha*I and M·*Taq*I are printed in bold and the following symbols are used for modified nucleosides: 2, 2-aminopurine-1-β-D-2′-deoxynucleoside; C^{Me}, 5-methyl-2′-deoxycytidine and A^{Me}, 6-methyl-2′-deoxyadenosine.

Fluorescence data processing

All fluorescence emission spectra and fluorescence intensities from titrations were corrected for protein tryptophan fluorescence by subtraction of control spectra and control titrations, where the 2-aminopurine fluorophor was replaced by adenine in the duplex oligodeoxynucleotides. In addition, fluorescence data were corrected for variable background emission of the solutions. This was necessary, because the 2-aminopurine fluorescence is highly quenched in duplex oligodeoxynucleotides and its fluorescence intensity at low duplex concentration used in this study (20 and 250 nM) is small compared with the background. Therefore, the fluorescence intensities of the various duplex oligodeoxynucleotides were measured at higher concentrations (typically between 0.5 and 4 μM). Fluorescence intensities of all duplex oligodeoxynucleotides containing 2-aminopurine showed a linear dependence on their concentrations. Fluorescence intensities at 20 and 250 nM concentration free of background were calculated from the obtained slopes. Titration data (fluorescence intensities as a function of total enzyme concentrations) were fitted to the real solution of the quadratic binding equation for one binding site (51) using the data analysis program GraFit (52).

RESULTS

Duplex oligodeoxynucleotides used

For fluorescence measurements with M·*Hha*I, which catalyses the methylation of the first cytosine within the ds 5′-G**C**GC-3′ DNA sequence, we used three hemimethylated duplex oligodeoxynucleotides, which are derived from the recognition sequence (for abbreviations of duplex oligodeoxynucleotides see Table 1). In G**2**GC the target cytosine, in 2**C**GC its 5′-neighbour and in G**C**2G its 3′-neighbour, is replaced with the fluorescent base 2-aminopurine. Since the recognition sequence of M·*Hha*I is palindromic, M·*Hha*I can, in principle, bind in two orientations. In order to direct binding of M·*Hha*I in the orientation, in which 2-aminopurine (G**2**GC) or cytosine (2**C**GC and G**C**2C) is targeted, the complementary strand in these duplexes contained 5-methylcytosine at the other target position. Such a preference for single binding orientation was observed in cocrystals of M·*Hha*I with hemimethylated DNA (53).

Analogous hemimethylated duplex oligodeoxynucleotides were used for the fluorescence measurements with M·*Taq*I, which catalyses the methylation of the adenine within the ds 5′-TCG**A**-3′ DNA sequence. In the duplex oligodeoxynucleotides TCG**2** and TC2**A** the target adenine and its 5′-neighbour are replaced by 2-aminopurine, whereas in TCG**A**2 2-aminopurine occupies the 3′-neighbour position outside the recognition sequence. In order to direct binding in the desired orientation the complementary strands in these duplex oligodeoxynucleotides contained N6-methyladenine at the other target position.

The various duplex oligodeoxynucleotides containing 2-aminopurine showed quite different fluorescence intensities (Table 2). In general, the fluorescence intensities of duplex oligodeoxynucleotides, in which the 2-aminopurine base can form a Watson–Crick-like base pair with thymine, are lower than those having 2-aminopurine in a mismatch position. Apart from base pairing, the 2-aminopurine fluorescence in these duplex oligodeoxynucleotides is also quite sensitive to the sequence context.

Table 2. Fluorescence intensities of duplex oligodeoxynucleotides containing 2-aminopurine before and after titration with M·*Hha*I or M·*Taq*I[a]

	Duplex containing 2-aminopurine	Fluorescence before titration (a.u.)	Fluorescence after titration (a.u.)	Relative fluorescence increase
1	G**2**GC	4.76 ± 0.04	255.3 ± 3.1	53.6 ± 2.1
2	2**C**GC	5.91 ± 0.05	8.7 ± 0.8	1.5 ± 0.2
3	G**C**2C	9.90 ± 0.40	18.0 ± 1.5	1.8 ± 0.2
4	TCG**2**	1.77 ± 0.06	23.0 ± 0.8	13.0 ± 0.9
5	TC2**A**	5.81 ± 0.27	9.9 ± 0.2	1.7 ± 0.1
6	TCG**A**2	4.45 ± 0.07	9.0 ± 0.1	2.0 ± 0.1

[a]For the fluorescence titrations with M·*Hha*I (rows 1–3) and M·*Taq*I (rows 4–6) duplex oligodeoxynucleotides containing 2-aminopurine-1-β-D-2′-deoxynucleoside (2) were used at 250 nM concentration and the excitation and emission wavelengths were set to 320 and 381 nm, respectively. Fluorescence intensities are given in arbitrary units (a.u.) and errors as standard deviations.

Binding of M·*Hha*I and M·*Taq*I to duplex oligodeoxynucleotides

Binding of M·*Hha*I and M·*Taq*I to the various duplex oligodeoxynucleotides was analysed in gel mobility shift assays. The results obtained with M·*Hha*I are shown in Figure 1. Duplex oligodeoxynucleotides were incubated with M·*Hha*I and the free duplex oligodeoxynucleotides (lower bands) separated from the M·*Hha*I-bound duplexes (upper bands) by non-denaturing gel electrophoresis. Under these conditions M·*Hha*I completely bound to G**2**GC, partly to the specific duplex oligodeoxynucleotide G**C**GC and no binding was observed with 2**C**GC and G**C**2G (lanes 1–4). However, addition of *S*-adenosyl-L-homocysteine (AdoHcy) to the incubation mixture resulted in nearly complete binding of all duplex oligodeoxynucleotides (lanes 5–8). Binding of M·*Taq*I to specific duplex oligodeoxynucleotide TCG**A** and the various duplex oligodeoxynucleotides containing 2-aminopurine is demonstrated in Figure 2. The electrophoretic mobilities of the duplex oligodeoxynucleotides alone are shown in lanes 1, 3, 5 and 7. Addition of M·*Taq*I (30 nM) prior to electrophoresis resulted in nearly complete formation of complexes for all four duplex oligodeoxynucleotides even in the absence of AdoHcy (upper bands in

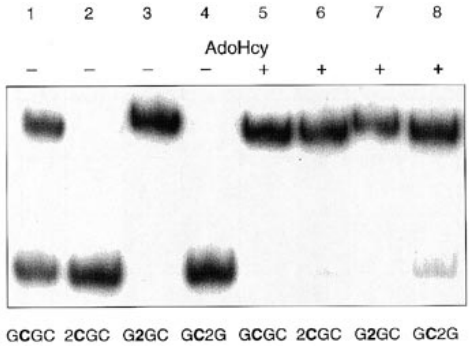

Figure 1. Gel mobility shift analysis of the interactions between M·*Hha*I (50 nM) and duplex oligodeoxynucleotides (5 nM). Lanes 1–4 in the absence and lanes 5–8 in the presence of 100 μM *S*-adenosyl-L-homocysteine (AdoHcy).

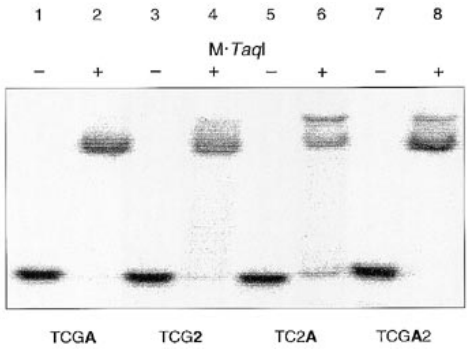

Figure 2. Gel mobility shift analysis of the interactions between M.*Taq*I and duplex oligodeoxynucleotides (1 nM). Lanes 1, 3, 5 and 7 in the absence of M.*Taq*I and lanes 2, 4, 6 and 8 in the presence of M.*Taq*I (30 nM).

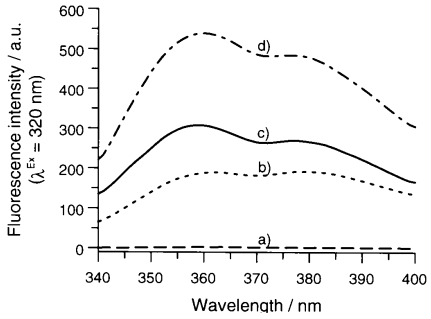

Figure 3. Fluorescence emission spectra of G**2**GC: curve (**a**) 250 nM duplex oligodeoxynucleotide alone, curve (**b**) 10 µM duplex oligodeoxynucleotide alone, curve (**c**) 250 nM duplex oligodeoxynucleotide in the presence of saturating concentration of M·*Hha*I (2 µM) and curve (**d**) 250 nM duplex oligodeoxynucleotide after digestion with DNase I and phosphodiesterase.

lanes 2, 4, 6 and 8). Gel mobility shift experiments with different M·*Taq*I concentrations showed that with increasing M·*Taq*I concentrations the ratio between complexes with lower mobility and complexes with higher mobility changed in favour of the complexes with lower mobility (data not shown). These results suggest that the complexes with lower mobility may represent complexes in which multiple M·*Taq*I molecules are bound to the duplex oligodeoxynucleotides.

Fluorescence studies with M·*Hha*I

Fluorescence spectra of G**2**GC, which places the 2-aminopurine fluorophor at the target site of M·*Hha*I, are shown in Figure 3. The 2-aminopurine fluorescence intensity of G**2**GC is very low at the concentration used in this study (curve a), but can be readily observed at higher levels (curve b). This is due to a very strong quenching of the fluorophor, which mainly results from stacking interactions with the neighbouring bases. The degree of fluorescence quenching in G**2**GC was determined by digestion with DNase I and phosphodiesterase. Enzymatic degradation of the duplex and release of the free 2-aminopurine-2′-deoxynucleotide (curve d) leads to a 100-fold increase of the fluorescence intensity at 381 nm. Upon addition of saturating amounts of M·*Hha*I to G**2**GC the 2-aminopurine fluorescence intensity at 381 nm increases 54-fold (Fig. 3, curve c and Table 2). Furthermore, the shape of the fluorescence emission spectrum in the presence of M·*Hha*I is changed compared with the duplex spectrum, but resembles that of the free 2-amino-

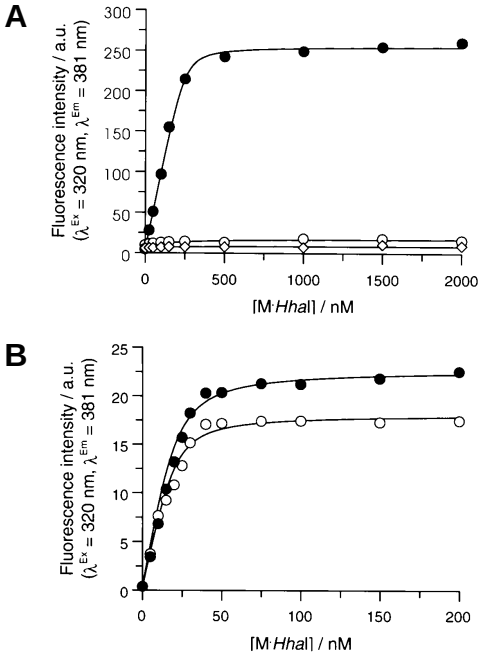

Figure 4. (**A**) Fluorescence titrations of G**2**GC (●), 2**C**GC (◇) and G**C**2C (○) at 250 nM concentration each with M·*Hha*I. Titrations of 2**C**GC and G**C**2C were done in the presence of *S*-adenosyl-L-homocysteine (50 µM). (**B**) Fluorescence titrations of G**2**GC at 20 nM concentration in the absence (●) and presence of 50 µM *S*-adenosyl-L-homocysteine (○) with M·*Hha*I. Data fitting yielded dissociation constants K_d of 3.9 ± 1.1 and 2.9 ± 0.9 nM in the absence and presence of *S*-adenosyl-L-homocysteine, respectively.

purine-2′-deoxynucleotide. This can be seen in Figure 3 by comparing the fluorescence emission spectrum of G**2**GC at 10 µM concentration (curve b) with those of G**2**GC at 250 nM concentration in the presence of M·*Hha*I and after enzymatic digestion (curves c and d, respectively). The emission spectrum of G**2**GC in the presence of M·*Hha*I shows a maximum at 359 nm, which is very close to the maximum of the free 2-aminopurine-2′-deoxynucleotide at 360 nm. Figure 4A shows a titration curve of G**2**GC with M·*Hha*I. The fluorescence signal reaches saturation within the concentration range used. However, because of the high concentration of G**2**GC (250 nM) used no accurate dissociation constant, K_d, could be determined in this experiment. Titrations with 20 nM G**2**GC (Fig. 4B) yielded K_d of 3.9 ± 1.1 and 2.9 ± 0.9 nM in the absence and presence of AdoHcy, respectively, which agrees well with the values determined in gel mobility shift assays (S. Serva and S. Klimasauskas, unpublished data).

The duplex oligodeoxynucleotides bearing 2-aminopurine at the 5′- (2**C**GC) and 3′-neighbouring (G**C**2C) positions behaved very differently. Since the gel mobility shift analysis (Fig. 1) indicates that M·*Hha*I binds these duplex oligodeoxynucleotides only when AdoHcy is added, fluorescence titrations were performed in the presence of AdoHcy (Fig. 4A). However, addition of M·*Hha*I to the 2**C**GC or G**C**2C duplex oligodeoxynucleotides leads only to very small fluorescence increases (1.5- and 1.8-fold, respectively).

Fluorescence studies with M·*Taq*I

Titrations of duplex oligodeoxynucleotides containing 2-aminopurine with M·*Taq*I are shown in Figure 5, and the relative fluorescence changes are listed in Table 2. Addition of saturating amounts of M·*Taq*I to the duplex oligodeoxynucleotide TCG**2**,

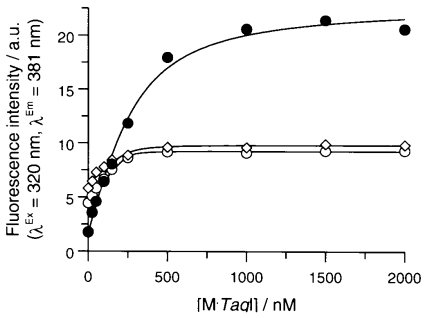

Figure 5. Fluorescence titrations of TCG**2** (●), TC2**A** (◇), TCG**A**2 (○) at 250 nM concentration each with M·*Taq*I. Data fitting of the titration with TCG**2** yielded a K_d of 120 ± 30 nM.

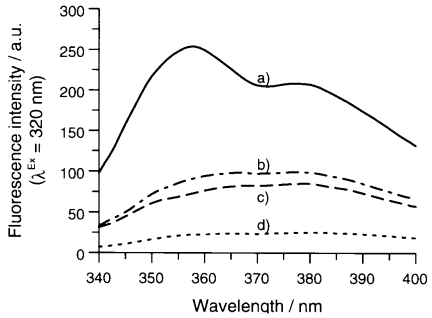

Figure 6. Fluorescence emission spectra of duplex oligodeoxynucleotides (2.5 μM): curve (**a**) TCG**2** in the presence of M·*Taq*I (7.5 μM), curve (**b**) TC2**A** in the presence of M·*Taq*I (7.5 μM), curve (**c**) TCG**A**2 in the presence of M·*Taq*I (7.5 μM) and curve (**d**) TCG**2** alone.

which carries the 2-aminopurine fluorophor at the target site of M·*Taq*I, results in a 13-fold increase of the fluorescence intensity. The titration data were fitted to the real solution of the quadratic binding equation for one binding site and resulted in a K_d of 120 ± 30 nM. This relatively weak binding is in conflict with the apparent tighter binding in the gel mobility shift assay (Fig. 2). Therefore, binding of M·*Taq*I to TCG**2** was measured in a third independent assay. The intrinsic tryptophan fluorescence of M·*Taq*I increases upon binding of M·*Taq*I to specific DNA. Titration of M·*Taq*I with TCG**2** at an excitation wavelength of 295 nm and an emission wavelength of 340 nm also results in a fluorescence increase (data not shown), which is highly dominated by the protein tryptophan fluorescence. This titration yielded a K_d of 120 ± 16 nM, which agrees very well with the K_d determined by 2-aminopurine fluorescence titration. Given the similarities of the K_d determined in the different fluorescence solution assays, we think that the gel mobility shift assay indicates too tight binding for M·*Taq*I. Fluorescence emission spectra of TCG**2** at 10-fold higher concentrations (2.5 μM) in the absence and the presence of saturating amounts of M·*Taq*I are shown in Figure 6. The shape of the emission spectrum of TCG**2** in the presence of M·*Taq*I (curve a) differs from the duplex spectrum (curve d), but resembles that of the free 2-aminopurine-2′-deoxynucleotide in Figure 3 (curve a). This is very similar to the result obtained for G**2**GC in the presence of M·*Hha*I. However, the emission spectrum of the M·*Taq*I–TCG**2** complex has a maximum of 357 nm and is slightly blue-shifted compared with the emission maximum of the free 2-aminopurine-2′-deoxynucleotide at 360 nm.

Titrations of the duplex oligodeoxynucleotides TC2**A** and TCG**A**2, in which the neighbouring bases of the target adenine are replaced by 2-aminopurine, lead only to 1.7- and 2.0-fold increases of the 2-aminopurine fluorescence intensity, respectively. Figure 6 also includes fluorescence spectra of TC2**A** (curve b) and TCG**A**2 (curve c) at 2.5 μM in the presence of saturating amounts of M·*Taq*I. In contrast with the M·*Taq*I–TCG**2** complex, complexes between M·*Taq*I and duplexes carrying 2-aminopurine at the neighbouring positions (TC2**A** and TCG**A**2) show fluorescence emission spectra with a shape similar to those of the duplex oligodeoxynucleotides alone (data not shown).

DISCUSSION

We have used the C5-cytosine DNA methyltransferase M·*Hha*I as a paradigm for a DNA base flipping enzyme. It was demonstrated by X-ray crystallography of a series of ternary complexes between M·*Hha*I, various versions of substrate DNA and the product cofactor AdoHcy that the enzyme flips its target cytosine out of the DNA and into its active site (1,53–55). In addition, there is indirect evidence that base flipping does also occur in the binary M·*Hha*I–DNA complex. It was shown, that M·*Hha*I catalyses exchange of the proton at the 5-position of cytosine with solvent in the absence of cofactor (56). Base flipping in the binary complex is also supported by the observation that M·*Hha*I binds more tightly to duplex oligodeoxynucleotides containing thymine, uracil (20) and even adenine or guanine replacements for the target cytosine (21). This enhanced binding of M·*Hha*I to such duplexes is attributed to the lower energy required for opening a mismatched base pair upon formation of the binary complex. Recently, base flipping in the binary complex has been observed by ^{19}F NMR spectroscopy (57). 2-Aminopurine also forms a mismatch with guanine in the G**2**GC duplex, and it is therefore not surprising that M·*Hha*I binds strongly to this duplex oligodeoxynucleotide in the gel shift assay.

Since base flipping results in a complete removal of the stacking interactions between the target base and its neighbours, and the fluorescence quenching of the 2-aminopurine base in dsDNA is mainly due to base stacking interactions, the 2-aminopurine fluorescence should increase dramatically if the 2-aminopurine base is flipped out of the DNA helix. Thus, the observed 54-fold increase of the 2-aminopurine fluorescence intensity upon addition of saturating amounts of M·*Hha*I to the duplex G**2**GC, in which the target cytosine is replaced by 2-aminopurine, is consistent with the 2-aminopurine base being flipped out of the double helix in the binary complex. The observation that the shape of the 2-aminopurine emission spectrum in the M·*Hha*I–G**2**GC complex is changed compared with the duplex spectrum but resembles that of the free 2-aminopurine-2′-deoxynucleotide, is also in agreement with an extrahelical 2-aminopurine in the binary complex. In addition, this may indicate that the flipped out 2-aminopurine base is solvent accessible to a quite large extent and that it is not locked in the catalytic pocket of the enzyme as was observed for the target base in the X-ray structures (1,53–55). It is indeed quite difficult to imagine how a much bulkier 2-aminopurine could replace cytosine in the active site pocket. Moreover, a lower electrophoretic mobility in the presence of AdoHcy of this complex compared with those containing cytosine at the target position (Fig. 1) indicates that this complex is less compact and suggests that the enzyme may not have undergone the complete conformational rearrangement of the active site loop required for catalysis (21). The absence of an

effect of AdoHcy on the electrophoretic mobility of this complex could be related to our observation that the dissociation constants of G**2**GC in the presence and absence of AdoHcy are not significantly different (Fig. 4B). It should be pointed out that duplex oligonucleotides with cytosine at the target position do show an increased binding upon addition of AdoHcy in gel mobility shift experiments (21). The insensitivity of the K_d of G**2**GC to the addition of AdoHcy could be due to the sterically more demanding 2-aminopurine base at the target position, which does not allow an AdoHcy-induced conformational rearrangement of M·*Hha*I to increase binding.

In contrast with G**2**GC, the duplex oligodeoxynucleotides 2**C**GC and G**C**2C, in which the neighbouring bases of the target cytosine are replaced with 2-aminopurine, bound to M·*Hha*I only in the presence of AdoHcy in the gel shift assay and gave only small increases of the 2-aminopurine fluorescence emission upon titration with M·*Hha*I (1.5- and 1.8-fold, respectively). In these complexes base flipping of the target cytosine should lead to a 2-aminopurine which has lost its base stacking interactions to one of its neighbours. This situation can be compared with duplex oligodeoxynucleotides having 2-aminopurine at the 3′-end. Bloom *et al.* (32) showed that placing 2-aminopurine at the 3′-end of a duplex oligodeoxynucleotide results in a very low fluorescence intensity and thus only one stacking neighbour is sufficient to result in a large fluorescence quenching (25- to 125-fold depending on the nature of the 5′-neighbour of 2-aminopurine). Therefore, the small fluorescence increases in the M·*Hha*I–2**C**GC and M·*Hha*I–G**C**2C complexes are in accordance with the neighbouring cytosine being flipped out of the DNA helix.

M·*Hha*I does not bend its DNA substrate significantly (1,58) and the large 2-aminopurine fluorescence intensity of the M·*Hha*I–G**2**GC complex can solely be attributed to base flipping. Since the 2-aminopurine fluorescence in duplex oligodeoxynucleotides is highly quenched due to stacking interactions with neighbouring bases, DNA bending, kinking and base flipping induced by DNA binding proteins should have different effects on the 2-aminopurine fluorescence intensity. In general, smooth bending does not result in an unstacking of neighbouring base pairs and thus should not lead to a large increase of the 2-aminopurine fluorescence. In contrast, kinking of DNA, as observed in DNA complexes with the catabolite gene activator protein (CAP) (59), the TATA-box binding protein (TBP) (60,61) or the restriction endonuclease *Eco*RV (62), leads to unstacking of adjacent base pairs (63). This leads to a situation, in which each base at the kink has only one stacking neighbour and may be compared with the M·*Hha*I–2**C**GC and M·*Hha*I–G**C**2C complexes, in which 2-aminopurine has only one stacking neighbour due to base flipping, or to a duplex oligodeoxynucleotide, in which 2-aminopurine is placed at the end. Since the later arrangements do not lead to a large 2-aminopurine fluorescence increase, DNA kinking is also not expected to result in a large fluorescence increase. Only if both stacking neighbours are removed upon DNA binding, e.g. by base flipping, duplex oligodeoxynucleotides containing 2-aminopurine should show a large fluorescence increase. However, it should be noted, that a small 2-aminopurine fluorescence increase due to bending or kinking might also give a valuable fluorescence signal change, which can be used to study DNA binding.

Titrations of duplex oligodeoxynucleotides containing 2-aminopurine with the adenine-specific DNA methyltransferase M·*Taq*I lead to similar results as those with M·*Hha*I. Replacement of the target adenine with 2-aminopurine within the recognition sequence of M·*Taq*I (TCG**2**) yields a strongly enhanced 2-aminopurine fluorescence signal (13-fold) upon titration with M·*Taq*I. In addition, the shape of the 2-aminopurine fluorescence emission spectrum in the M·*Taq*I–TCG**2** complex resembles that of the free 2-aminopurine-2′-deoxynucleotide. Addition of M·*Taq*I to duplex oligodeoxynucleotides bearing 2-aminopurine at the 5′-neighbouring position (TC2**A**) or at the 3′-neighbouring position (TCG**A**2) of the target adenine show only a 1.7- and 2.0-fold increase of the fluorescence intensity, respectively. In addition, the shapes of the fluorescence emission spectra are similar to those of the duplex oligodeoxynucleotides alone. The similarities of the results obtained with M·*Hha*I and M·*Taq*I strongly indicate a common base flipping mechanism for both DNA methyltransferases.

The lower fluorescence intensity of the M·*Taq*I–TCG**2** complex compared with the M·*Hha*I–G**2**GC complex might be explained by different chemical environments of the 2-aminopurine base when flipped out of the DNA helix. It was suggested for M·*Taq*I, that the target adenine after being flipped out of the DNA will interact with NPPY (105–108), VVP (164–166) and F196 in the M·*Taq*I–DNA complex (17). Since the 2-aminopurine quantum yield is reduced in hydrophobic solvents (29) and the putative active site of M·*Taq*I is very hydrophobic, a reduced 2-aminopurine fluorescence intensity is expected. In addition, the 2-aminopurine fluorescence is blue-shifted in hydrophobic solvents (29) and the observed 3 nm blue shift of the 2-aminopurine emission maximum in the M·*Taq*I–TCG**2** complex compared with the free 2-aminopurine-2′-deoxynucleotide supports this interpretation. Alternatively, the lower fluorescence intensity of the M·*Taq*I–TCG**2** complex could be explained by different equilibria between an inner- and extrahelical state of the 2-aminopurine base in the M·*Taq*I–TCG**2** and M·*Hha*I–G**2**GC complexes. 2-Aminopurine can form two Watson–Crick-like hydrogen bonds to the partner thymine in the TCG**2** duplex, whereas in G**2**GC 2-aminopurine forms a mismatch with the partner guanine. Therefore, the equilibrium in the M·*Hha*I–G**2**GC complex could lie more on the extrahelical side compared with that in the M·*Taq*I–TCG**2** complex, which could explain the higher 2-aminopurine fluorescence intensity of the M·*Hha*I–G**2**GC complex. A third explanation for the lower fluorescence of the M·*Taq*I–TCG**2** complex could be that a certain fraction of the enzyme docks to the recognition sequence in the alternative orientation which does not lead to a flipped out 2-aminopurine base. However, this possibility can be excluded, because in studies with a duplex oligodeoxynucleotide, in which the target bases of both strands were replaced with 2-aminopurine, no higher fluorescence intensity is observed upon addition of M·*Taq*I compared with the M·*Taq*I–TCG**2** complex (data not shown).

Recently, fluorescence studies with duplex oligodeoxynucleotides containing 2-aminopurine and the N6-adenine DNA methyltransferase M·*Eco*RI have been reported (43). Similar to our results with M·*Hha*I and M·*Taq*I, addition of stoichiometric amounts of M·*Eco*RI to a duplex oligodeoxynucleotide containing 2-aminopurine at the target site resulted in a large (14-fold) increase of the 2-aminopurine fluorescence. These findings with M·*Taq*I and M·*Eco*RI give experimental evidence that a base flipping mechanism similar to that described for the C5-cytosine DNA methyltransferases M·*Hha*I and M·*Hae*III also operates in adenine-specific DNA methyltransferases. Since the active site residues of M·*Taq*I as well as other amino acids are highly conserved among N6-adenine DNA methyltransferases and N4-cytosine DNA methyltransferases (18,19,64), a common base flipping mechanism for all DNA

methyltransferases seems likely (5). This hypothesis can now be tested experimentally by using duplex oligodeoxynucleotides, in which the target base is replaced by 2-aminopurine.

In conclusion, the C5-cytosine DNA methyltransferase M·*Hha*I, which is known to flip out its target base for catalysis, leads to a large increase of the 2-aminopurine fluorescence when added to duplex oligodeoxynucleotides containing 2-aminopurine at the target site. Addition of the N6-adenine DNA methyltransferase M·*Taq*I to duplex oligodeoxynucleotides, in which the target base is replaced by 2-aminopurine, also results in a strongly enhanced 2-aminopurine fluorescence emission. These results demonstrate that 2-aminopurine can be used as a fluorescence probe for DNA base flipping. In addition, this approach is suitable to determine K_d in the nanomolar range. Furthermore, it should be possible to use the 2-aminopurine fluorescence signal in stopped flow experiments to monitor DNA base flipping in real time.

ACKNOWLEDGEMENTS

We would like to thank Jack Benner and Cheryl Baxa from New England Biolabs for providing the M·*Taq*I expression vector and Nathalie Bleimling for the purification of M·*Taq*I. We also would like to thank Roger Goody for his continuous support and Bernard Connolly for carefully reading the manuscript. This work was supported by a grant from the Deutsche Forschungsgemeinschaft and from the Volkswagen-Stiftung.

REFERENCES

1 Klimasauskas,S., Kumar,S., Roberts,R.J. and Cheng,X. (1994) *Cell*, **76**, 357–369.
2 Reinisch,K.M., Chen,L., Verdine,G.L. and Lipscomb,W.N. (1995) *Cell*, **82**, 143–153.
3 Vassylyev,D.G., Kashiwagi,T., Mikami,Y., Ariyoshi,M., Iwai,S., Ohtsuka,E. and Morikawa,K. (1995) *Cell*, **83**, 773–782.
4 Slupphaug,G., Mol,C.D., Kavli,B., Arvai,A.S., Krokan,H.E. and Tainer,J.A. (1996) *Nature*, **384**, 87–92.
5 Roberts,R.J. (1995) *Cell*, **82**, 9–12.
6 Moore,M.H., Gulbis,J.M., Dodson,E.J., Demple,B. and Moody,P.C.E. (1994) *EMBO J.*, **13**, 1495–1501.
7 Vrielink,A., Rüger,W., Driessen,H.P.C. and Freemont,P.S. (1994) *EMBO J.*, **13**, 3413–3422.
8 Mol,C.D., Kuo,C.-F., Thayer,M.M., Cunningham,R.P. and Tainer,J.A. (1995) *Nature*, **374**, 381–386.
9 Park,H.-W., Kim,S.-T., Sancar,A. and Deisenhofer,J. (1995) *Science*, **268**, 1866–1872.
10 Thayer,M.M., Ahern,H., Xing,D., Cunningham,R.P. and Tainer,J.A. (1995) *EMBO J.*, **14**, 4108–4120.
11 Yamagata,Y., Kato,M., Odawara,K., Tokuno,Y., Nakashima,Y., Matsushima,N., Yasumura,K., Tomita,K., Ihara,K., Fujii,Y., Nakabeppu,Y., Sekiguchi,M. and Fujii,S. (1996) *Cell*, **86**, 311–319.
12 Labahn,J., Schärer,O.D., Long,A., Ezaz-Nikpay,K., Verdine,G.L. and Ellenberger,T.E. (1996) *Cell*, **86**, 321–329.
13 Gong,W., O'Gara,M., Blumenthal,R.M. and Cheng,X. (1997) *Nucleic Acids Res.*, **25**, 2702–2715.
14 McClelland,M. (1981) *Nucleic Acids Res.*, **9**, 6795–6804.
15 Labahn,J., Granzin,J., Schluckebier,G., Robinson,D.P., Jack,W.E., Schildkraut,I. and Saenger,W. (1994) *Proc. Natl. Acad. Sci. USA*, **91**, 10957–10961.
16 Schluckebier,G., Labahn,J., Granzin,J., Schildkraut,I. and Saenger,W. (1995) *Gene*, **157**, 131–134.
17 Schluckebier,G., O'Gara,M., Saenger,W. and Cheng,X. (1995) *J. Mol. Biol.*, **247**, 16–20.
18 Klimasauskas,S., Timinskas,A., Menkevicius,S., Butkienè,D., Butkus,V. and Janulaitis,A. (1989) *Nucleic Acids Res.*, **17**, 9823–9832.
19 Malone,T., Blumenthal,R.M. and Cheng,X. (1995) *J. Mol. Biol.*, **253**, 618–632.
20 Yang,A.S., Shen,J.-C., Zingg,J.-M., Mi,S. and Jones,P.A. (1995) *Nucleic Acids Res.*, **23**, 1380–1387.
21 Klimasauskas,S. and Roberts,R.J. (1995) *Nucleic Acids Res.*, **23**, 1388–1395.
22 Cal,S. and Connolly,B.A. (1997) *J. Biol. Chem.*, **272**, 490–496.
23 Millar,D.P. (1996) *Curr. Opin. Struct. Biol.*, **6**, 322–326.
24 McLaughlin,L.W., Leong,T., Benseler,F. and Piel,N. (1988) *Nucleic Acids Res.*, **16**, 5631–5644.
25 Connolly,B.A. (1991) In Eckstein,F. (ed.) *Oligonucleotides and Analogues: A Practical Approach*. IRL Press, Oxford, pp. 155–183.
26 Connolly,B.A. (1992) *Methods Enzymol.*, **211**, 36–53.
27 Schmidt,S. and Cech,D. (1995) *Nucleosides Nucleotides*, **14**, 1445–1452.
28 Fujimoto,J., Nuesca,Z., Mazurek,M. and Sowers,L.C. (1996) *Nucleic Acids Res.*, **24**, 754–759.
29 Ward,D.C., Reich,E. and Stryer,L. (1969) *J. Biol. Chem.*, **244**, 1228–1237.
30 Guest,C.R., Hochstrasser,R.A., Sowers,L.C. and Millar,D.P. (1991) *Biochemistry*, **30**, 3271–3279.
31 Xu,D., Evans,K.O. and Nordlund,T.M. (1994) *Biochemistry*, **33**, 9592–9599.
32 Bloom,L.B., Otto,M.R., Beechem,J.M. and Goodman,M.F. (1993) *Biochemistry*, **32**, 11247–11258.
33 Hochstrasser,R.A., Carver,T.E., Sowers,L.C. and Millar,D.P. (1994), *Biochemistry*, **33**, 11971–11979.
34 Bloom,L.B., Otto,M.R., Eritja,R., Reha-Krantz,L.J., Goodman,M.F. and Beechem,J.M. (1994) *Biochemistry*, **33**, 7576–7586.
35 West Frey,M., Sowers,L.C., Millar,D.P. and Benkovic,S.J. (1995) *Biochemistry*, **34**, 9185–9192.
36 Marquez,L.A. and Reha-Krantz,L.J. (1996) *J. Biol. Chem.*, **271**, 28903–28911.
37 Újvári,A. and Martin,C.T. (1996) *Biochemistry*, **35**, 14574–14582.
38 Jia,Y., Kumar,A. and Patel,S.S. (1996) *J. Biol. Chem.*, **271**, 30451–30458.
39 Sastry,S.S. and Ross,B.M. (1996) *Biochemistry*, **35**, 15715–15725.
40 Dunkak,K.S., Otto,M.R. and Beechem,J.M. (1996) *Anal. Biochem.*, **243**, 234–244.
41 Raney,K.D., Sowers,L.C., Millar,D.P. and Benkovic,S.J. (1994) *Proc. Natl. Acad. Sci. USA*, **91**, 6644–6648.
42 Bjornson,K.P., Moore,K.J.M. and Lohman,T.M. (1996) *Biochemistry*, **35**, 2268–2282.
43 Allan,B.W. and Reich,N.O. (1996) *Biochemistry*, **35**, 14757–14762.
44 Roberts,R.J., Myers,P.A., Morrison,A. and Murray,K. (1976) *J. Mol. Biol.*, **103**, 199–208.
45 Mann,M.B. and Smith,H.O. (1979) In Usdin,E., Borchardt,R.T. and Creveling,C.R. (eds), *Proceedings of the Conference on Transmethylation*. Elsevier, New York, pp. 483–492.
46 Andrus,A. (1992) *Evaluating and Isolation Synthetic Oligonucleotides*. Applied Biosystems.
47 Kumar,S., Cheng,X., Pflugrath,J.W. and Roberts,R.J. (1992) *Biochemistry*, **31**, 8648–8653.
48 Laemmli,U.K. (1970) *Nature*, **227**, 680–685.
49 Schluckebier,G., Kozak,M., Bleimling,N., Weinhold,E. and Saenger,W. (1997) *J. Mol. Biol.*, **265**, 56–67.
50 Bradford,M.M. (1976) *Anal. Biochem.*, **72**, 248–254.
51 Reinstein,J., Vetter,I.R., Schlichting,I., Rösch,P., Wittinghofer,A. and Goody,R.S. (1990) *Biochemistry*, **29**, 7440–7450.
52 Leatherbarrow,R.J. (1992) *GraFit Version 3.0*, Erithacus Software Ltd., Staines, UK.
53 O'Gara,M., Roberts,R.J. and Cheng,X. (1996) *J. Mol. Biol.*, **263**, 597–606.
54 O'Gara,M., Klimasauskas,S., Roberts,R.J. and Cheng,X. (1996) *J. Mol. Biol.*, **261**, 634–645.
55 Kumar,S., Horton,J.R., Jones,G.D., Walker,R.T., Roberts,R.J. and Cheng,X. (1997) *Nucleic Acids Res.*, **25**, 2773–2783.
56 Wu,J.C. and Santi,D.V. (1987) *J. Biol. Chem.*, **262**, 4778–4786.
57 Klimasauskas,S., Szyperski,T., Serva,S., Wüthrich,K. (1998) *EMBO J.*, **17** 317–324.
58 García,R.A., Bustamante,C.J. and Reich,N.O. (1996) *Proc. Natl. Acad. Sci. USA*, **93**, 7618–7622.
59 Schultz,S.C., Shields,G.C. and Steitz,T.A. (1991) *Science*, **253**, 1001–1007.
60 Kim,Y., Geiger,J.H., Hahn,S. and Sigler,P.B. (1993) *Nature*, **365**, 512–520.
61 Kim,J.L., Nikolov,D.B. and Burley,S.K. (1993) *Nature*, **365**, 520–527.
62 Winkler,F.K., Banner,D.W., Oefner,C., Tsernoglou,D., Brown,R.S., Heathman,S.P., Bryan,R.K., Martin,P.D., Petratos,K. and Wilson,K.S. (1993) *EMBO J.*, **12**, 1781–1795.
63 Travers,A.A. (1991) *Curr. Opin. Struct. Biol.*, **1**, 114–122.
64 Timinskas,A., Butkus,V. and Janulaitis,A. (1995) *Gene*, **157**, 3–11.